

Observation of a low-symmetry crystal structure for superconducting MgCNi_3 by Ni K -edge x-ray absorption measurements

A. Yu. Ignatov,¹ L. M. Dieng,¹ T. A. Tyson,¹ T. He,² and R. J. Cava²¹*Department of Physics, New Jersey Institute of Technology, Newark, New Jersey 07102*²*Department of Chemistry and Princeton Material Institute, Princeton University, Princeton, New Jersey 08544*

(Received 7 December 2001; revised manuscript received 16 September 2002; published 28 February 2003)

The local atomic structure of MgCNi_3 has been determined over the temperature range of 3 to 300 K by Ni K -edge x-ray absorption fine structure measurements. No anomalies were observed near $T_c \sim 7$ K. However, below $T^* \sim 70$ K the symmetry of Ni_6 octahedra is lower than the cubic $Pm-3m$ determined by conventional diffraction measurements. We suggest that the onset of local distortions could be closely related with removal of the degeneracy in the electronic states dominated by the Ni d bands. The results are discussed in relation to nuclear magnetic resonance, x-ray photoemission measurements, and the superconductivity.

DOI: 10.1103/PhysRevB.67.064509

PACS number(s): 74.70.Dd, 78.70.Dm, 61.10.Ht

I. INTRODUCTION

The recently discovered MgCNi_3 intermetallic compound with superconducting transition temperature $T_c \sim 7$ K (Ref. 1) would not have been viewed as a likely candidate for superconductivity. The conduction electrons are derived from partially filled Ni d states, which typically leads to ferromagnetism in metallic Ni and many Ni-based binary alloys. The electronic structure of MgCNi_3 was studied using local density functional calculations.²⁻⁵ The states near the Fermi level were found to be dominated by Ni d character. However, the Stoner factor is strongly reduced compared to that in pure Ni due to hybridization with C and is not large enough to induce a ferromagnetic ground state. Neutron powder diffraction^{1,6(a)} showed no ferromagnetic ordering down to 2 K.

The crystal structure of MgC_xNi_3 is the simple cubic perovskite structure, space group $Pm-3m$,^{1,6(a),6(b)} and the lattice parameter a is 3.812 Å at $x \sim 0.97$ and ambient temperature.^{1,6(a)} The structure is a simple perovskite with the carbon atom at the body-center position, surrounded by a cage of six Ni atoms at the face-center positions, with eight Mg atoms occupying the cube corners. The lattice parameter and the neutron scattering derived Debye-Waller factors smoothly increase with temperature with no anomalies found in temperature range of 2 to 295 K.^{6(a)} Perovskites often exhibit symmetry-lowering transitions on cooling. Structural anomalies could be ordered over a short range that is much smaller than the coherence length of conventional diffraction measurements. Accurate information on the *local structure* of MgCNi_3 is vital for the following reasons. As mentioned above, the density of states in the vicinity of the Fermi level is dominated by Ni d bands. Most of those bands are very narrow, since they do not disperse about many points of high symmetry in the simple cubic Brillouin zone.⁴ Degeneracy in the band structure could be lifted by small perturbations, such as an electron-phonon interaction coupling the degenerate states, or lowering of the symmetry from cubic through a Peierls type transition. The covalent character of the Ni-C bond implies that though most of amplitude of the electron wave function resides on the Ni d there might be spatial

distribution of charge and/or spin governed by the strength of Ni-C hybridization, Coulomb, and electron-phonon interactions.⁷ It is possible that the charge/spin distribution within Ni-C bonds is not periodic. In fact, neutron diffraction refinement^{1,6(a)} did not reveal lattice distortions (long range), which might be associated with charge density waves (CDW's), nor long-range antiferromagnetic (AF) ordering, which is constituent to spin density waves (SDW's). However, upper critical field measurements suggests a very short coherence length $\xi \sim 45$ Å (Ref. 8) that is clearly on atomic length scales. Therefore, it is worth investigating MgCNi_3 for formation of local charge density waves (LCDW's) and local spin density waves (LSDW's) by using local-structure sensitive techniques. Recent results of nuclear magnetic resonance (NMR) (Ref. 9) are consistent with enhancement of spin fluctuations as the temperature decreases. The work reported here is undertaken to determine whether or not there are any local structural distortions in MgCNi_3 as the signature of possible LCDW's/LSDW's.

The experimental technique emphasized in this work is an extended x-ray absorption fine structure (EXAFS) which provides local structural information on atomic length scales about selected atomic sites. Relevant to the present work, Ni K -edge EXAFS measurements have been undertaken. First three shells (C, Ni, and Mg) were analyzed and the interatomic distances and Debye-Waller (DW) factors were determined in a broad range of temperatures between 3.2 and 300 K. Once the structural data were extracted they were considered in light of recent experimental observations^{1,8-11} aiming at answering the following questions. (i) Are there any structural instabilities near T_c ? (ii) Is there any other specific temperature (range of temperatures) where structural changes take place? (iii) Are there phonon anomalies (softening of optical vibration mode or anharmonicity)? (iv) Are there correlations between local structural changes and transport properties, showing that the structural changes are related to electronic properties?

The experimental details and the results of fitting of EXAFS data are given in Sec. II. Neither the interatomic distances nor the DW factors showed evidence for anomalies near T_c . However, broadness of all the above pair distribu-

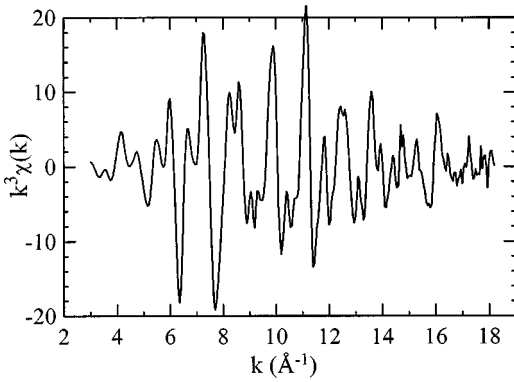


FIG. 1. $\chi(k)*k^3$ of MgCNi_3 from the Ni K -edge EXAFS at 3.2 K.

tions, even at very low temperatures, prompted our search for possible local distortions from the perfect single-site distributions associated with cubic $Pm-3m$ lattice. We begin Sec. IV by introducing an anharmonic pair vibration potential for Ni-Ni pairs and will be showing that the potential evolves from the double-well (multiple-well) below 70 K to the anharmonic single well above 200 K. The results are discussed in relation to NMR (Ref. 9) and transport measurements,^{1,10,11} to illustrate that the local distortions observed in this work is a signature of the LSDW's and/or LSDW's. The implications for x-ray photoemission measurements as well as to the superconductivity are discussed.

II. EXPERIMENTAL METHODS

A polycrystalline sample of MgCNi_3 was prepared at Princeton University as described in Ref. 1. Samples from the same batch have been recently characterized by powder neutron diffraction, four-probe resistivity, dc magnetization,¹ tunneling,⁸ and nuclear magnetic resonance (NMR) (Ref. 9) measurements that enable us to discuss the EXAFS results in a light of previous findings (Sec. IV).

The x-ray absorption spectra were measured between 3.2 and 300 K, with temperature monitored within ~ 0.2 (1.0) K below (above) 20 K. Data were collected on beamline X-11A of the National Synchrotron Light Source, using a Si(111) monochromator. The higher-energy harmonics were suppressed by detuning the second crystal of the double-crystal monochromator on its rocking curve to $\frac{1}{2}$ of maximum intensity at ~ 1 KeV above the edge. Ni K -edge spectra of MgCNi_3 and Ni metal foil were recorded simultaneously in transmission mode. The latter were used to bring all data for MgCNi_3 on the same absolute energy scale, which was calibrated by assigning $E=8333$ eV to first inflection point of the Ni foil. From two to five scans were collected for each temperature to ensure reproducibility of the data. The EXAFS data were reduced according to the standard procedure.¹² A typical $\chi(k)$ spectrum weighted by k^3 is shown in Fig. 1 demonstrating good data quality up to 17.7 \AA^{-1} .

III. RESULTS

Magnitudes of Fourier transformed (FT) $\chi(k)k^3$ at several temperatures are shown in Fig. 2. The first and second peaks

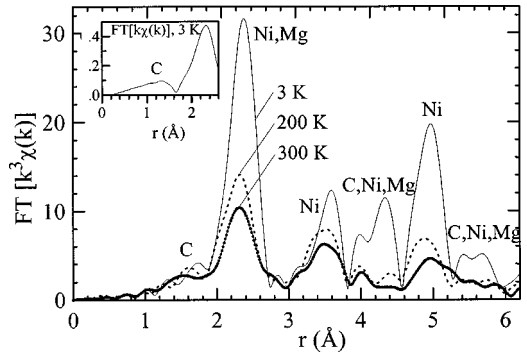


FIG. 2. Magnitude of the Fourier transform (FT) of $\chi(k)*k^3$ for MgCNi_3 at 3, 200, and 300 K. The data are transformed with a square window between $3.3\text{--}17.7 \text{ \AA}^{-1}$. The insert is to show a clear contribution due to Ni-C pairs.

at about 1.6 and 2.2 \AA are due to single scattering of the photoelectron by two carbon atoms (in shell at $\sim 1.6 \text{ \AA}$) and eight nickel and four magnesium atoms (in shells at $\sim 2.2 \text{ \AA}$). In the simple cubic perovskite structure the Ni-Ni and Ni-Mg bond lengths are expected to be equal. More distant Ni-X neighbors are evident in the low-temperature data. However, they contain contributions of multiple scattering (MS) paths and will not be treated in this paper.

EXAFS from the Ni-Ni and Ni-Mg shells were isolated by back Fourier transformation (BFT) to k space over the range of $\sim 1.83\text{--}2.87 \text{ \AA}^{-1}$ (square window). The resulting data were fit over the range of 4–15 \AA in terms of a two-shell model, allowing the interatomic distances, DW factors, and energy shifts to vary freely while keeping Ni-Ni and Ni-Mg coordination numbers at 8 and 4. Amplitudes and phase shifts were generated by the FEFF-6 code¹³ using the crystalline structure from Ref. 1. Although a good fit was achieved, the Ni-Mg distance fell into a false minimum at 2.82 \AA —too long compared to 2.70 \AA predicted by diffraction. Therefore, we constrained the Ni-Mg bondlength to 2.70 \AA . It should be mentioned that this constraint limits possible local distortions of Ni-Mg bonds to a single-site distribution. However, it is still well-motivated in the EXAFS analysis: Since the Mg is a light scatterer, the Ni-Mg contribution is a very minor addition to the Ni-Ni signal for $k > 6 \text{ \AA}^{-1}$ (i.e., over most of the fitting range of 4–15 \AA^{-1}) and for the DW factors above 0.005 \AA^2 . In the fit of 3.2 K data, where the lowest broadening is expected, the DW factors for the Ni-Ni and Ni-Mg bonds were estimated at ~ 0.006 and 0.007 \AA^2 , respectively. Both values are in the range where $\sigma^{(2)}k^2 > 1$ above $k \sim 13 \text{ \AA}^{-1}$ and application of DW factors *alone* is no longer accurate to reconstruct the pair distribution functions (PDF's).

Moderate non-Gaussian disorder can be modeled by a cumulant expansion.^{14,15} The second cumulant is the conventional DW factor. The third and fourth cumulants (C_3 and C_4), if positive, give rise to a high- r tail and symmetrical redistribution of the PDF's weight from its center into the wings. In the EXAFS spectrum, C_3 affects the phase shift $\phi(k) = \phi_0(k) - 4/3k^3C_3$, while C_4 rescales the magnitude $A(k) = A_0(k) * \exp(2/3k^4C_4)$. The Cumulant expansion converges rapidly, and therefore can be truncated at n th term

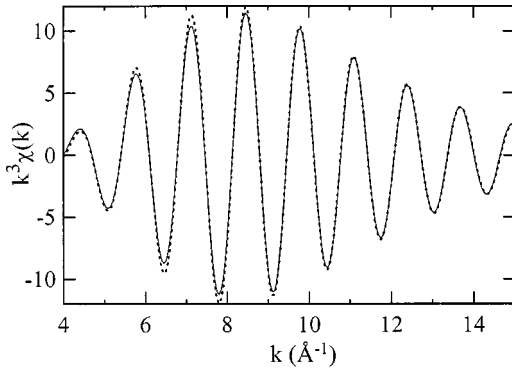


FIG. 3. Comparison of the Fourier-filtered data (solid line) with model involving Ni-Ni and Ni-Mg pairs (dashed line) at 3.2 K. Dot-dashed curve ($\theta_E=211$ K, $\Delta\sigma^2=0.0023$ Å², and $C_4=1.1 \times 10^{-5}$ Å⁴) provides a satisfactory fit for the entire temperature range. Parameters of the model are given in Table I. The BFT transform range is 1.83–2.87 Å, square window.

provided that $k^{n+2}C_{n+2} \ll k^n C_n < 1$. Further through the fit, due to the reason mentioned above, the Ni-Mg distribution modeled by a harmonic distribution ($C_n=0$, for $n>2$). For the Ni-Ni distribution, the C_3 and C_4 were allowed to vary. As revealed from Fig. 3, excellent fit to the filtered data was achieved for $\sigma^{(2)} \equiv C_2 = (6.3 \pm 0.5) \times 10^{-3}$ Å², $C_3 = (-0.5 \pm 1.5) \times 10^{-5}$ Å³, and $C_4 = (1.1 \pm 0.3) \times 10^{-5}$ Å⁴. C_5 and C_6 cumulants were found to be negligible. Structural parameters for several temperatures are summarized in Table I. As revealed from the fits, no significant changes in mean Ni-Ni distances were observed over the entire temperature range. Extracted distances agree within the error bars with those derived from the diffraction data. The DW factor and cumulant C_4 increase with temperature as is shown in Figs. 4 and Fig. 5, with no anomalies near T_c . Except for 300 K, $k^4 C_4 < 1$, so that the cumulant series for Ni-Ni distribution is convergent over the range of 4–15 Å⁻¹. Note, that C_4 saturates

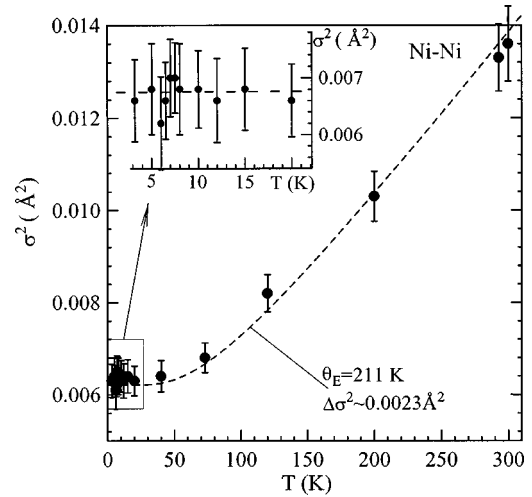


FIG. 4. Temperature dependence of Debye-Waller factor of the Ni-Ni bond. Solid curve ($\theta_E=211$ K, $\Delta\sigma^2=0.0023$ Å²) provides a satisfactory fit for the experimental dependence. As seen in the insert, the DW factor is unchanged across T_c .

at $T^* \leq 70$ K rather than tending to zero at $T \rightarrow 0$ as expected in a slightly anharmonic single-well potential. Both Ni-Ni and Ni-Mg pair distributions are surprisingly broad, implying a local distortion from the perfect single-site distributions associated with the cubic $Pm\bar{3}m$ lattice. Possible origins and types of the distortions will be discussed in Sec. IV.

To analyze the Ni-C pair distribution, we started from $\chi(k)$ weighted by k . This emphasizes the Ni-C peak in the FT with respect to the Ni-Ni peak enabling the BFT to k space over the range of ~ 0.98 – 1.76 Å (square window). Single-shell fits were done over the range of 4–14 Å⁻¹. The Ni-C interatomic distance was found to be 1.90 ± 0.01 Å in the whole temperature range, in good agreement with the diffraction data. The carbon coordination number and DW factor are strongly correlated. The data can be nicely fit as

TABLE I. Local structural parameters of Ni-Ni pair as a function of temperature. Further details of the fit $S_0^2=0.9$. Numbers of Ni and Mg neighbors are fixed at 8 and 4 in accordance with the diffraction data. The Ni-Mg interatomic distance is constrained to 2.70 Å with only a harmonic distribution considered. All but C_4 cumulants are found to be negligible for Ni-Ni PDF. For the ranges of fit of 4–15 Å⁻¹ in k space and 1.83–2.87 Å in r space, the allowed number of fitting parameters is 9.¹⁶ The total number of the parameters used in this fit is 6. The estimated errors are ~ 0.01 Å in Ni-Ni distance, $\sim 10\%$ in DW factor, and $\sim 30\%$ in C_4 . The temperature dependence of the DW factors and C_4 with error bars generated by the fit are shown in Figs. 3–5. The overall quality of the fit is illustrated in Fig. 3. Diffraction results from Ref. 6(a) are given for comparison.

T (K)	Ni K -edge EXAFS				Diffraction, Ref. 6(a)	
	R (Å)	$\sigma^{(2)}$ (Å ²)	$C_4 \times 10^5$ (Å ⁴)	a (Å)	U_{\parallel}/U_{\perp} (Å ²)	
3.2	2.68	0.0063	1.14	3.8065	0.0038/0.0050	
6.0	2.68	0.0061	0.67			
8.0	2.68	0.0064	0.83			
20	2.68	0.0063	0.97	3.8066	0.0038/0.0048	
40	2.68	0.0064	1.11			
73	2.68	0.0068	1.15			
120	2.68	0.0082	1.63			
200	2.67	0.0103	1.80	3.8095	0.0049/0.0094	
300	2.67	0.0136	4.30	3.8125	0.0061/0.0118	

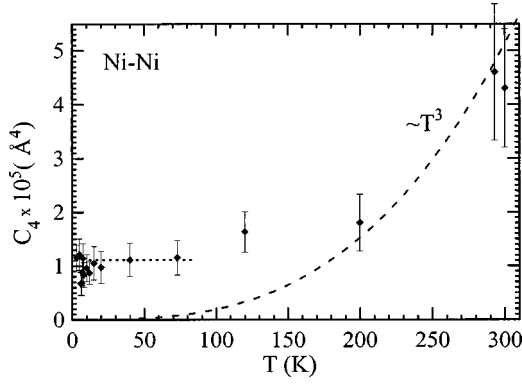


FIG. 5. Fourth cumulant of the Ni-Ni distribution as function of temperature. Above 200 K the cumulant follows T^3 (dashed line) that is expected (Ref. 15) for slightly anharmonic potential $W(r) = \frac{1}{2}\varphi(r-r_0)^2 + \frac{1}{24}\phi(r-r_0)^4$ with $\varphi > 0$ and $\phi < 0$ (high-temperature anharmonic). Note that the low-temperature points fall well above the dashed line.

suming a coordination number between 1.4 and 2.2, suggesting (as expected) that EXAFS has low sensitivity to carbon stoichiometry compared to neutron diffraction on MgC_xNi_3 .¹ Further, we fixed the number of nearest-neighbor carbons to 2.0 and extracted temperature dependence of the DW factor is shown in Fig. 6 by diamonds. For most points of interests $\sigma^{(2)}k_{\text{max}}^2 < 1$, so that the harmonic approximation appears to be sufficient. The large absolute value of broadening ($\sim 0.0052 \text{ \AA}^2$ at 10 K) for the short Ni-C distance ($\sim 1.9 \text{ \AA}$) comes either from large Debye vibration frequency of the pair ($\theta_D \sim 516 \text{ K}$, dashed line in Fig. 6) or from more than one interatomic distances characterized by correlated motion of Ni-C pairs. To explore the latter, a variety of constrained fits keeping the total carbon coordination number of 2.0 but allowing two different Ni-C bonds and corresponding two different DW factors were attempted. None of the models

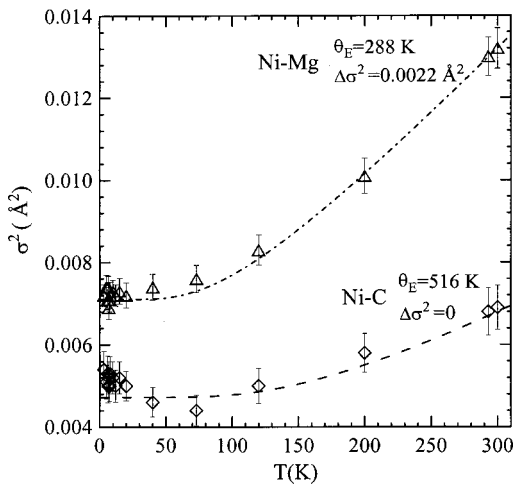


FIG. 6. Debye-Waller factors of the Ni-C and Ni-Mg bonds vs temperature. Both factors are unchanged across T_c . The Einstein model with $\theta_E = 516 \text{ K}$ and $\Delta\sigma^2 = 0$ (dashed line) fits to the Ni-C bond dependence. The temperature dependence of the Ni-Mg bond could be fit by an Einstein model assuming $\theta_E = 288 \text{ K}$ that is shifted by $\Delta\sigma^2 = 0.0022 \text{ \AA}^2$.

improves the quality of fit parameter, which accounts for number of degrees of freedom in the fit. Therefore, Ni K -edge data do not provide supporting evidences for local breathing-type distortions of the Ni-C bonds. An estimate for an upper limit for such distortions will be given in Sec. IV B.

IV. DISCUSSION

Since electronic states at Fermi level are of mostly Ni d -type²⁻⁵ we will focus on the Ni-Ni pair distribution. The positive C_4 gives rise to a redistribution of PDF spectral weight from its center to the wings. We note that the identical PDF is achieved when two equivalent Gaussian peaks are slightly moved apart, signifying the trend towards a split of Ni-Ni pair distribution. An accurate description of C_4 vs T would require detail information on lattice dynamic that has not been reported yet. Alternatively, we adopted numerical parametrization of the Ni-Ni PDF (Ref. 17) utilizing an effective pair potential $W(r)$.¹⁸

A. Analysis of Ni-Ni PDF using anharmonic pair potential

The Ni-Ni PDF has a non-Gaussian shape (C_4 is not small) and Ni-Ni pairs move in anharmonic pair potential. Considering for simplicity a polynomial of degree four:

$$W(r) = C + 1/2\varphi(T)(r-r_0)^2 + 1/6\gamma(T)(r-r_0)^3 + 1/24\phi(T)(r-r_0)^4 \quad (1)$$

that is well suited for describing a broad range of pair motion from almost harmonic single-well ($\varphi \gg \gamma$ and $\varphi \gg \phi$) to essentially anharmonic double well ($\varphi < 0$ and $\phi > 0$). The Ni-Ni pair distribution function $g(r)$ was obtained numerically, in a quantum approximation, using eigenvalues (E_i) and eigenfunctions (Ψ_i) of a stationary Schrödinger equation with the interatomic potential $W(r)$ (Ref. 18)

$$g(r) = \frac{\sum_i |\Psi_i(r)|^2 \exp(-E_i/kT)}{\sum_i \exp(-E_i/kT)}. \quad (2)$$

The model EXAFS function due to the Ni-Ni pairs was obtained as

$$\chi(k) = NS_0^2 \text{Im} \left\{ B(k, r_0) \int \frac{g(r) \exp\{i[2kr + 2\delta(k, r_0)]\}}{kr^2} dr \right\}, \quad (3)$$

where the amplitude $B(k, r_0)$ and phase shift $\delta(k, r_0)$ were calculated using the FEFF-6.¹³ It was added to the model EXAFS due to the Ni-Mg pairs and fit to experimental EXAFS from the Ni-Ni and Ni-Mg pairs. The Ni-Mg structural parameters, BFT window, and range of fit in the k space were the same as in Sec. III. The $\varphi(T)$ and $\phi(T)$ were allowed to vary at each temperature point, while the $\gamma(T)$ was set to zero because of the symmetry of the Ni-Ni PDF.

Extracted temperature dependencies of φ and ϕ are shown in Fig. 7. The polynomial reduces to a typical double-well

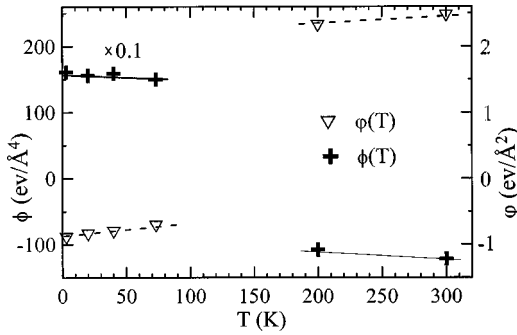


FIG. 7. Temperature dependence of parameters φ and ϕ governing the anharmonic potential $W(r)$. The low-temperature region of ϕ is shown reduced by factor of 10. Note the crossover in the potential parameters as one goes from low to high temperature region, implying that a structural phase transition takes place somewhere between $T^* \sim 70$ and 200 K.

potential $\{\varphi < 0, \phi > 0, \text{ and } C = 3/2\varphi^2/\phi \text{ [to keep } V(r_0 \pm \Delta) = 0]\}$ at $T \leq 70$ K. Above 200 K the experimental data cannot be described by the double-well potential. Instead, the fit returns $\varphi > 0, \phi < 0, \text{ and } C = 0$ that is a signature of anharmonic single-well potential. Interpretation in the range of 70–200 K is not straightforward (where the sample likely consists of at least two microscopic phases) and is a subject of microscopic model that is beyond the scope of this paper. However, what is apparent from the Fig. 7 is that, the anharmonic model exhibits a crossover behavior somewhere between 70 and 200 K.

The crossover brings about an excessive broadening of the Ni-Ni pair distribution

$$\Delta\sigma_{\text{ex}}^{(2)} = \int g(r, W)(r - \langle r_w \rangle)^2 dr - \int g(r, V)(r - \langle r_v \rangle)^2 dr, \quad (4)$$

where $g(r, W)$ and $g(r, V)$ are PDF's calculated in the quantum approximation [Eq. (2)] for anharmonic $W(r)$ [Eq. (1)] and harmonic $V(r) = K/2(r - r_0)^2$ potentials. The $\langle r_w \rangle$ and $\langle r_v \rangle$ correspond to mean Ni-Ni distances in $W(r)$ and $V(r)$, respectively. $V(r)$ represents a potential to which the high-temperature anharmonic potential $W(r, T \sim 200\text{--}300$ K) would have diverged if an anharmonic term ϕ were disappearing with decreasing temperature. The spring constant was evaluated from Fig. 7, as an average of $\varphi(T)$ over the range 200–300 K, yielding $K = 2.3 \pm 0.3$ eV/Å². The excessive broadening is plotted in Fig. 8 along with temperature dependencies of the ¹³C NMR Knight shift (open rhombs) reported by Singer *et al.*⁹ Within the error bars of the both experimental techniques the Knight shift is directly proportional to the excessive broadening ${}^{13}K(T) = \alpha \Delta\sigma_{\text{ex}}^{(2)}(T)$ with $\alpha \sim 6.7 \pm 0.4$ Å⁻². The ${}^{13}K(T)$ changes curvature from positive to negative at about 120 K (Ref. 9) that is in the same T range where the structural crossover takes place, Fig. 7. Therefore, temperature dependence of the uniform spin susceptibility follows the temperature dependence of the excessive broadening somewhat below 120 K.

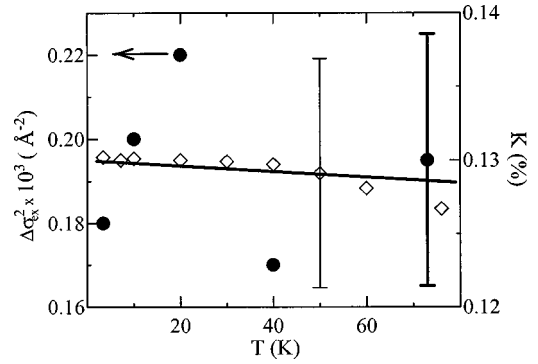


FIG. 8. Comparison of temperature dependence of the excessive broadening obtained from EXAFS data by using Eq. (4) with the temperature dependence of ¹³C Knight shift reported by Singer *et al.*⁹ Solid line representing a least square fit of the $\Delta\sigma_{\text{ex}}^{(2)}$ data over the range of this figure matches the $K(T)$ dependence.

B. Estimate for Ni displacements

A recent neutron diffraction study suggests anisotropic motion of the Ni atom characterized by displacements that are twice as large perpendicular to the C-Ni bond compared to displacements along the bond (Table I). Possible rotation of Ni₆ octahedra has been put forward.⁴ However, it is noteworthy that rigid rotation *alone* does not broaden the Ni-Ni distribution. To gain the distortions in Ni-Ni PDF, the *symmetry of Ni₆ octahedra must be lowered* to tetragonal, orthorhombic or possibly monoclinic, and, therefore, the rigid rotation must be combined with breathing or half-breathing (stretching) displacement modes. Our estimates for the possible Ni atom displacements from their original position in cubic $Pm\bar{3}m$ are based upon the fact that the ultimate purpose of EXAFS is to reconstruct PDF. Structural models having the same PDF's must have same EXAFS functions [see Eq. (2)]. We will simulate the Ni-Ni distribution determined in Sec. III ($R_0 = 2.68$ Å, $N = 8$, $\sigma^{(2)} = 0.0063$ Å², and $C_4 = 1.1 \times 10^{-5}$ Å⁴ at $T = 3.2$ K) assuming two and three groups of Ni-Ni distances. DW factors for slightly different bonds will be considered the same and equal to the residual of purely dynamic part with $\theta_E \sim 211$ K [$\sigma^{(2)}(\theta_E = 211; T \rightarrow 0) \sim 0.004$ Å²]. In this way our estimate yields typical splitting in Ni-Ni distances, which may be locally gained at the expense of $\Delta\sigma^{(2)} \sim 0.0023$ Å² and $C_4 \sim 1.1 \times 10^{-5}$ Å⁴.

From Ni K -edge EXAFS analyzed up to $k_{\text{max}} = 15$ Å⁻¹ (Ref. 17) we have placed upper limits for the Ni displacements at $\sim 0.02(0.05)$ Å for full(half) breathing distortions of Ni-C bond and at ~ 0.05 Å for the displacements perpendicular to the Ni-C bond. Since the displacements are less than thermal vibrations the potentials overlap forming a multiple-well potential (the double-well potential considered in Sec. IV A for simplicity).

C. Exploring analogies between Ba_{1-x}K_xBiO₃ and MgCNi₃

It is instructive to begin with recalling major structural results provided by long-range order sensitive techniques and details of LDA calculations presumed long-range order periodicity. Neutron diffraction measurements show that both

$\text{Ba}_{1-x}\text{K}_x\text{BiO}_3$ (BKBO) ($x > 0.37$) (Ref. 19) and MgCNi_3 (Refs. 1, 6(a)) have a cubic $Pm-3m$ unit cell in temperature range of 3–300 K implying that the O_6 and Ni_6 octahedra are undistorted. LDA band structure calculations regard BKBO and MgCNi_3 as cubic metals those electronic states about the Fermi energy are essentially O p (Ref. 20) and Ni d character.^{2–5} Most of the energy bands do not disperse about many points of high symmetry in the simple cubic Brillouin zone.⁴ These diffraction and LDA results enable one important observation: In both compounds, *electronic states at Fermi levels are dominated by partial density of states from elements constituting “perfect” octahedra and are degenerate*. The Jahn-Teller theorem asserts that a system having a degenerate ground state will spontaneously deform to lower its symmetry unless the degeneracy is simply a spin degeneracy.²¹ This causes an energy gap between the degenerate states to open up, lowering the electronic energy of the system.

Local sensitive EXAFS measurements²² indeed show that the BKBO ($x = 0.4$) structure is distorted from $Pm-3m$, possessing both tilting and breathing distortions of Bi-O bonds. A pseudogap observed in reflectivity spectra is about 0.5 eV.²³ Both experimental observations are attributed to the LCDW's that are well known to replace the CDW's in parent BaBiO_3 upon doping with K.¹⁹ The present EXAFS study clearly shows that in order to gain the observed distortions in Ni-Ni pair distribution (below $T^* \sim 70$ K) the symmetry of Ni_6 octahedra must be lower than cubic $Pm-3m$. Combining EXAFS, NMR,⁹ and transport¹⁰ data we would like to point out that the observation of structural, spin, and electronic crossovers between 50 and 200 K are consistent with formation of LCDW's and/or LSDW's. The correlation between local distortions and uniform spin susceptibility has been established in Sec. IV A. Transport measurements suggest that apart from T_c there is another characteristic transport temperature T_{tr}^* (or range of temperatures) between ~ 50 –140 K, depending on the measured response functions.^{1,9–11} Temperature dependence of electrical resistivity exhibits changes of curvature at 70–80 K. Between 80 and 300 K the $\rho(T)$ data can be fit to Bloch-Grüneisen law, assuming an Einstein temperature of ~ 200 K and obeys power law $\rho(T) \sim T^n$ with $n \sim 1.4$ at low temperatures.¹⁰ The Hall coefficient is small and negative showing that the normal state transport is mainly due to electrons, as in BKBO ($x = 0.4$). The Hall coefficient decreases from 300 to about 140 K followed by essentially temperature-independent behavior as temperature decreases.¹⁰ A two-band model involving light electrons and heavy holes has been put forward to explain temperature dependencies of the normal state resistivity and Hall coefficient.¹¹ It is worthwhile noting that in Refs. 5, 11 the holes are heavy due to the dispersion law in the nearly empty band of perfect $Pm-3m$ lattice, while the EXAFS results imply that the carrier mass gets enhanced as they couple to the local lattice distortions at $T^* \sim 70$ –200 K: The characteristic structural T^* and transport T_{tr}^* temperatures are in the same range showing that the *onset of the local distortions correlates with the electronic crossovers*.

An observation of the local lattice distortions (Sec. III) implies opening a gap (or pseudogap) and, therefore, a lower density of states in the vicinity of the Fermi energy than that estimated from the LDA calculations.^{2–4} High-resolution x-ray photoemission or reflectivity data are not yet available and are viewed as a critical test for LCDW's/LSDW's presence. New LSDA calculations minimizing a total energy of the MgCNi_3 supercell with respect to the displacements of Ni atoms are clearly motivated by the EXAFS findings.

Results of LDA calculations of MgCNi_3 (Refs. 2, 3) suggested that the conventional electron-phonon coupling is sufficient to produce the observed $T_c \sim 7$ K. However, the EXAFS data do not support two essential prepositions utilized for the T_c estimates, namely, assumptions of (i) a perfect and long-range ordered $Pm-3m$ structure and (ii) harmonic lattice vibrations. The former underestimates the nesting effects and, therefore, the charge/spin fluctuations that are enhanced through a spatial modulation of Ni d density of states for some segments of the Fermi surface. Charge and spin fluctuations could contribute to the pairing but they unlikely promote to the s -wave pairing²⁴ considering in Refs. 2 and 3. The latter cannot explain the excessive broadening of Ni-Ni pair distribution at $T^* \leq 70$ K that is not amenable to harmonic phonons. Importantly, the LCDW's/LSDW's occur at temperatures that are about 10 times larger than T_c and, therefore, they might possess sufficient energy to mediate the pairing of the light carriers. Along with conclusions of tunneling⁸ and NMR (Ref. 9) measurements we cannot rule out unconventional contribution to the pairing states.

V. CONCLUSIONS

We have reported details of the local structure of polycrystalline MgCNi_3 in the temperature range of 3.2–300 K. Ni K -edge EXAFS shows that Ni-C, Ni-Ni, and Ni-Mg interatomic distances are consistent with previous neutron diffraction results.¹ Neither the interatomic distances, nor the corresponding Debye-Waller factors behave anomalously near $T_c \sim 7$ K within the errors bars of, respectively, $\pm 0.01 \text{ \AA}$ and $\pm 0.0005 \text{ \AA}^2$ and the EXAFS data being analyzed up to $k_{\max} = 15 \text{ \AA}^{-1}$ (momentum transferred, $Q = 30 \text{ \AA}^{-1}$). The Ni-Ni distribution is found to be usually broad for a metallic compound $k^2 \sigma^{(2)} > 1$ and the conventional harmonic description is broken down. The cumulant approach^{14,15} was employed. We demonstrated that C_3 and further even cumulants are negligible, and, therefore, the Ni-Ni PDF is symmetric. To achieve convergence, it is sufficient to retain C_4 all but at 300 K. We found that C_4 saturates at $T^* \leq 70$ K rather than tending to zero at $T \rightarrow 0$. This disagrees with the behavior in a slightly anharmonic single-well potential.

Parameters of the anharmonic potential were evaluated working in the assumption that the Ni-Ni interatomic potential can be described using a polynomial of degree 4. Direct EXAFS fit to the experimental data indicates that the polynomial reduces to typical double-well potential at $T^* \leq 70$ K and to conventional single-well anharmonic potential at $T \geq 200$ K. Successful reconstruction of the polynomial coefficient illustrates the high selectivity of EXAFS technique to the interatomic potential and provides new means to

trace local structural transformations by looking into changes in the interatomic potential. The double-well potential implies displacements of $\Delta = \sqrt{-6\varphi/\phi} \sim 0.05$ Å. This value is in satisfactory agreement with an estimate based on the cumulant representation of Ni-Ni PDF placing the upper limits for Ni displacements at $\sim 0.02(0.05)$ Å for full (half) breathing distortions of Ni-C bond and at ~ 0.05 Å for the displacements perpendicular to the Ni-C bond.

We have considered the local structure of MgCNi₃ in connection to that of well-explored Ba_{0.6}K_{0.4}BiO₃ and noticed that (i) Ni₆(O₆) octahedra are locally distorted from those expected in perfect cubic *Pm-3m* and (ii) electronic states at the vicinity of Fermi level are mostly derived from the Ni *d* (*Op*) partial density of states and are *degenerate*. In Ba_{0.6}K_{0.4}BiO₃ the degeneracy is broken through oxygen-reside LCDW's. The anomalous properties of MgCNi₃ in its normal state⁹⁻¹¹ may be understood assuming the nickel-

residing LCDW's and/or LSDW's to remove the degeneracy in MgCNi₃. A microscopic model accounting for the intimate relationship between the electronic and lattice degrees of freedom needs to be developed.

ACKNOWLEDGMENTS

This work was supported by U.S. National Science Foundation (NSF) Career Grant No. DMR-9733862 and DMR-0209243. Work at Princeton University was funded by U.S. NSF and U.S. Department of Energy (DOE) through Grants No. DMR-9809483 and DE-FG02-98-ER45706. EXAFS data acquisition was performed at National Synchrotron Light Source, Brookhaven National Laboratory, which was supported by the U.S. DOE, Division of Materials Sciences and Division of Chemical Sciences under Contract No. DE-AC02-98CH10886.

-
- ¹T. He, Q. Huang, A. P. Ramirez, Y. Wang, K. A. Regan, N. Rogado, M. A. Hayward, M. K. Haas, J. S. Slusky, K. Inumara, H. W. Zandbergen, N. P. Ong, and R. J. Cava, *Nature (London)* **411**, 54 (2001).
- ²S. B. Dugdale and T. Jarlborg, *Phys. Rev. B* **64**, 100508 (2001).
- ³J. H. Shim, S. K. Kwon, and B. I. Min, *Phys. Rev. B* **64**, 180510(R) (2001).
- ⁴D. J. Singh and I. I. Mazin, *Phys. Rev. B* **64**, R140507 (2001).
- ⁵H. Rosner, R. Weht, M. D. Johannes, W. E. Pickett, and E. Tosatti, *Phys. Rev. Lett.* **88**, 027001 (2002).
- ⁶(a) Q. Huang, T. He, K. A. Regan, N. Rogado, M. A. Hayward, M. K. Haas, K. Inumaru, and R. J. Cava, *cond-mat/0105240* (unpublished); (b) For earlier synthesis and structural measurements on this system see B. Bogdanovik, K.-H. Claus, S. Gurtzen, B. Spliethoff, and U. Wilczok, *J. Less-Common Met.* **131**, 163 (1987).
- ⁷K. Yonemitsu, A. R. Bishop, and J. Lorenzana, *Phys. Rev. B* **47**, 8065 (1998).
- ⁸Z. Mao, M. M. Rosario, K. Nelson, K. Wu, I. G. Deac, P. Schiffer, Y. Liu, T. He, K. A. Regan, and R. J. Cava, *cond-mat/0105280* (unpublished).
- ⁹P. M. Singer, T. Imai, T. He, M. A. Hayward, and R. J. Cava, *Phys. Rev. Lett.* **87**, 257601 (2001).
- ¹⁰S. Y. Li, R. Fan, X. H. Chen, C. H. Wang, W. Q. Mo, K. Q. Ruan, Y. M. Xiong, X. G. Luo, H. T. Zhang, L. Li, Z. Sun, and L. Z. Cao, *Phys. Rev. B* **64**, 132505 (2001).
- ¹¹T. G. Kumary, J. Janaki, A. Mani, S. M. Jaya, V. S. Sastry, Y. Hariharan, T. S. Radhakrishnan, and M. C. Valsakumar, *cond-mat/0202277* (unpublished).
- ¹²T. M. Hayes and J. B. Boyce, in *Solid State Physics*, edited by H. Ehrenreich, F. Seitz, and D. Turnbull (Academic, New York, 1982), Vol. 37, p. 173.
- ¹³S. I. Zabinsky, J. J. Rehr, A. Ankudinov, R. C. Albers, and M. J. Eller, *Phys. Rev. B* **52**, 2995 (1995).
- ¹⁴G. Bunker, *Nucl. Instrum. Methods* **207**, 437 (1983).
- ¹⁵J. M. Tranquada and R. Ingalls, *Phys. Rev. B* **28**, 3520 (1983).
- ¹⁶E. A. Stern, *Phys. Rev. B* **48**, 9825 (1993).
- ¹⁷Possible models for Ni-Ni PDF will be discussed elsewhere. A. Yu. Ignatov and T. A. Tyson (unpublished).
- ¹⁸J. Mustre de Leon, S. D. Conradson, I. Batistic, A. R. Bishop, I. D. Raistrick, M. C. Aronson, and F. H. Garzon, *Phys. Rev. B* **45**, 2447 (1992).
- ¹⁹Shiyu Pei, J. D. Jorgensen, B. Dabrowski, D. G. Hinks, D. R. Richards, A. W. Mitchell, J. M. Newsam, S. K. Sinha, D. Vaknin, and A. J. Jacobson, *Phys. Rev. B* **41**, 4126 (1990).
- ²⁰L. F. Mattheiss and D. R. Hamann, *Phys. Rev. B* **28**, 4227 (1983).
- ²¹H. A. Jahn and E. Teller, *Proc. R. Soc. London, Ser. A* **161**, 234 (1937).
- ²²A. Yu. Ignatov, *J. Synchrotron Radiat.* **6**, 532 (1999); A. Yu. Ignatov, *Nucl. Instrum. Methods Phys. Res. A* **448**, 332 (2000).
- ²³S. H. Blanton, R. T. Collins, K. H. Kelleher, L. D. Rotter, Z. Schlesinger, D. G. Hinks, and Y. Zheng, *Phys. Rev. B* **47**, 996 (1993).
- ²⁴See, for example, Ref. 5, and references therein.